

Composite graphene/nanocarbons prepared by one-step reduction reaction

Nadia Todorova^{1,2*}, Vera Marinova¹, Dimitre Dimitrov^{1,3}, Christos Trapalis²

Institute of Optical Materials and Technologies, Bulgarian Academy of Science, bl. 109 "Acad. G. Bonchev" Str., 1113 Sofia, Bulgaria¹

Institute of Nanoscience and Nanotechnology, National Centre for Scientific Research "Demokritos", 15341 Athens, Greece²

Institute of Solid State Physics, Bulgarian Academy of Science, 72 Tzarigradsko Chaussee Blvd, 1784 Sofia, Bulgaria³

n.todorova@inn.demokritos.gr

Abstract: Nowadays, the decrease of CO₂ concentration in the atmosphere and/or its utilization need urgent resolution. At the same time, preparation of advanced graphene-based composites through effective environmentally benign procedures remains in the focus of intensive research. In the present work, composites consisted of reduced graphene oxide and nanocarbons (rGO/nC) were prepared by simultaneous reduction reaction of solid graphite oxide and CO₂ gas over alkaline earth reductant. The structure and the morphology of the prepared composite material were examined employing X-ray diffraction analysis and scanning electron microscopy. It was revealed that the characteristic narrow peak of the graphite oxide (GtO) at low 2θ (~11°) was not present in the pattern of the composite suggesting its successful reduction. Instead, a broad one positioned at 26° was recorded which was attributed to the formed nanocarbons. The observed accordion-like morphologies typical for reduced-graphene-oxide type of graphene evidenced the detachment of the graphene layers during the thermal treatment, while the formed nanocarbons were with irregular shape. The rGO/nC composite exhibited specific surface area (485 m²/g) higher than the pure nanocarbons (417 m²/g) obtained without addition of GtO. The outcome was attributed to the influence of the layered rGO which hinders the aggregation of the nanocarbons and facilitates their homogeneous distribution. The prepared composite can be considered as candidates for gas and energy storage applications, while the suggested environmentally benign preparation method can be scaled up to industrial extent due to simplicity.

Keywords: 2D COMPOSITES, REDUCED GRAPHENE OXIDE, NANOCARBONS, CO₂

1. Introduction

The development of graphene-containing composite materials remains in the focus of the research community due to the constantly increasing variety of application of this type of materials, but also due to the search for effective, scalable methods for their preparation [1, 2]. Graphene in the form of reduced graphene oxide (rGO) is often coupled with other carbonaceous materials such as carbon nanotubes, activated carbon, etc. in order functional properties like conductivity, specific surface area, stability etc. to be further improved. The main approaches for composite preparation are *in situ* synthesis of the second component in presence of rGO, as well as simultaneous decoration and reduction of the parent graphite oxide (GtO). Methods such as chemical reduction with suitable substances and thermal reduction in various gas or vacuum atmosphere, as well as combination of them are among the most used [3, 4].

On the other hand, the high concentration of greenhouse gases in the atmosphere, especially the CO₂ pollutant, needs to be urgently tackled. Metallothermic reduction of CO₂ to carbon nanostructures is one of the used methods which employs alkaline earth elements usually Mg as reductant [5]. Various modifications of the Mg and CO₂ precursors have been reported such as using additions of other metals like Zn and Ca to facilitate the CO₂ reduction [6], [7], but also using other substances for example silica, instead of the CO₂ in order to be reduced by the Mg under inert atmosphere [8].

In the present work, solid graphite oxide was added to Mg in order to be reduced by the metal along with the flowing CO₂ gas, aiming at preparation of composite rGO/nanocarbons in one-step GtO and CO₂ reduction reaction. The structural and morphological properties of the composite material were investigated in comparison with pure nanocarbons prepared in absence of GtO.

2. Experimental

2.1. Synthesis of the materials

The initial free-standing paper-like graphite oxide was prepared by oxidation of natural graphite applying a modified Hummers method as described in [9]. Then, the GtO was subjected to metallothermic treatment in CO₂ flow at conditions similar to those in [10]. In this experiment, a mixture of GtO and Mg powder in ratio 1:5 was placed in tube furnace onto an alumina scaffold and cured at 675 °C for 1 h under CO₂ flow. The heating up to the target temperature and the natural cooling after the reaction were

performed under Ar flow. Subsequently, the obtained powder was treated in boiling 3M HCl for 1 h under reflux and washed /centrifuged with deionized water until pH 7 in order the co-product MgO and the unreacted Mg to be removed. Finally, the solid material was dried at 80 °C overnight, collected and nominated as rGO/nC. For reference purpose, pure nanocarbons were prepared at the same conditions without addition of GtO which were named nC.

2.2. Characterization

The crystalline structure of the prepared pure and composite materials were investigated through XRD analysis employing Siemens D500 instrument with CuKα radiation source. The patterns were recorded in the 2θ range 2 - 70° with velocity 0.03°/s. SEM analysis was performed using FEI Inspect electron microscope with tungsten filament operating at 25 kV. The porosity of the materials was investigated using Quantachrome Autosorb-iQ instrument. Prior measurement, the samples were degassed at 120 °C for 12 h. The Brunauer-Emmett-Teller (BET) specific surface area and the total pore volume were determined from the liquid N₂ adsorption isotherms, while the pore size distribution was received from the desorption branch of the isotherms applying BJH analysis.

3. Results and discussion

The XRD patterns of the initial GtO, the intermediate rGO/nC before the acid treatment and washing, as well as the final pure nC and rGO/nC are presented in Fig. 1 and 2.

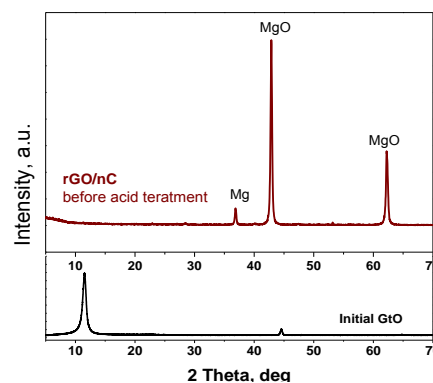


Fig. 1 XRD patterns of the initial graphite oxide (GtO) and the composite rGO/nC before the acid treatment.

It is evident that the narrow peak of the GtO at low $2\theta \sim 11^\circ$ is not present in the pattern of the intermediate (Fig. 1) and the final composite (Fig. 2). This outcome indicates that the initial GtO was either delaminated/reduced to rGO or its content in the composite is below the detection limit of the technique. Also, the well-defined peaks of MgO and Mg recorded for the intermediate composite were not present in the patterns of the final rGO/nC and pure nC, evidencing their successful removal by the acid treatment. Instead, a broad peak positioned at $\sim 26^\circ$ was recorded which was attributed to the (002) diffraction line of the formed nanocarbons [5].

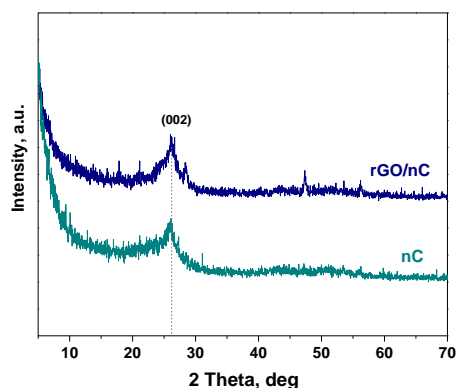


Fig. 2 XRD patterns of the final pure nanocarbons (nC) and composite material (rGO/nC).

The results from the SEM analysis presented in Fig. 3 and 4 are in good accordance with the XRD results. Specifically, from Fig. 3 it is evident that the stacked layers of the GtO (a and b) were detached after the metallothermic treatment resulting in accordion-like network (c and d) that is typical for thermally reduced graphene oxide [11]. The irregular aggregates in these images are attributed to carbon nanostructures together with the co-product MgO and non-reacted Mg.

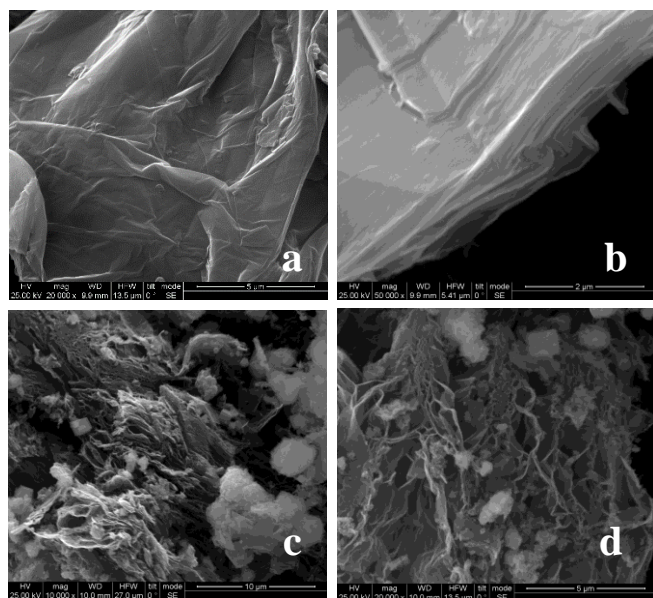


Fig. 3 SEM images of the initial graphite oxide (a, b) and the composite rGO/nC before acid treatment and washing (c, d).

In Fig. 4, SEM images of the composite rGO/nC and pure nC after the acid treatment and washing are given. For the composite, two types of morphologies, i.e. thin packs of layers and particles' aggregates can be observed, while for the pure nC only the second type is present. It can be expected that the rGO sheets will influence the porosity acting as a support for the *in-situ* formed nanocarbons. The fact that the rGO layers in the sample after the acid treatment

(Fig. 4 a and b) appear more detached in comparison to those before the treatment (Fig. 3 c and d) can be related to the influence of the hot HCl which reacts with the MgO and Mg and contribute to the rGO delamination and nanocarbons dispersion.

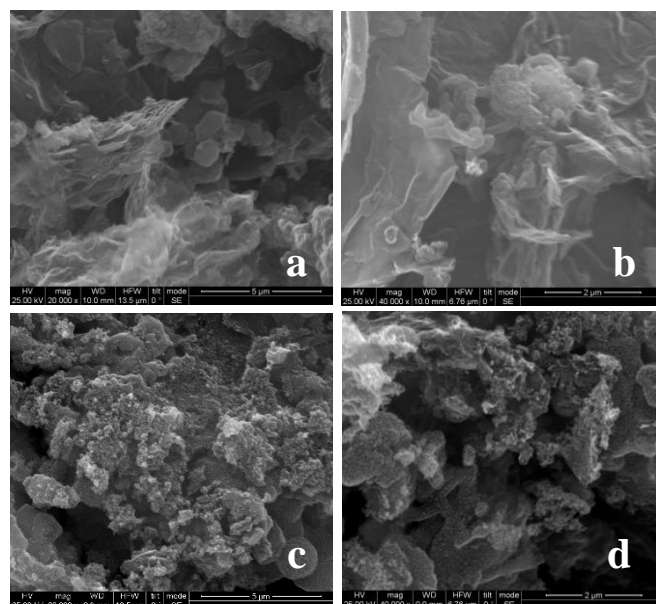


Fig. 4 SEM images of the final composite rGO/nC (a, b) the pure nanocarbons (c, d).

The performed liquid N_2 adsorption-desorption measurements verified the increase in the porosity of the composite rGO/nC in comparison to the initial GtO and pure nC sample. The isotherms and pore size distribution for the samples are presented in Fig. 4.

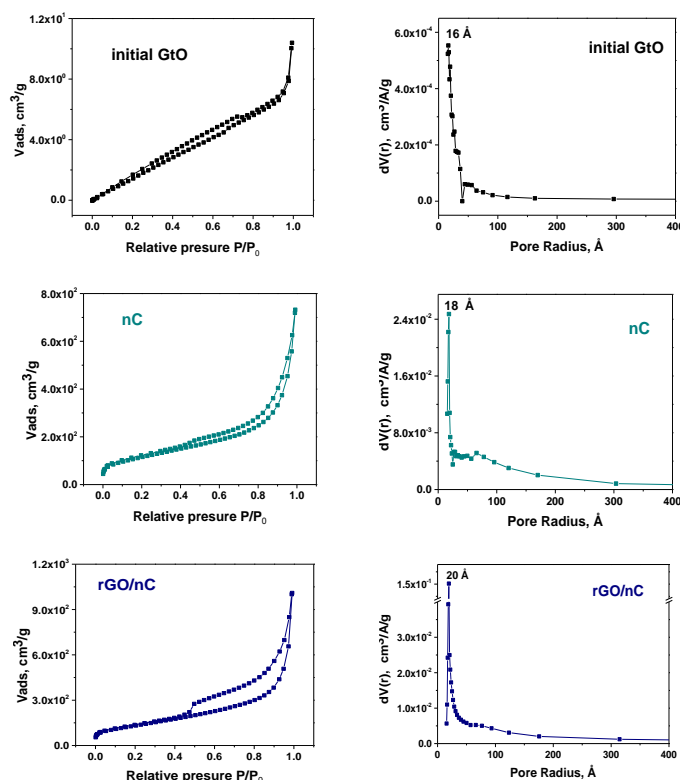


Fig. 5 Liquid N_2 adsorption-desorption isotherms and the pore size distribution plots of the initial graphite oxide (GtO), the pure nanocarbons (nC) and the composite rGO/nC.

The absorption branches can be categorized as type II and IV typical for makro- and mesoporous solids. The hysteresis loop formed due to different behavior in adsorption and desorption at the

same pressure P/P_0 matches H3 type, which is characteristic for materials consisted of aggregates from non-uniform particles forming slit shaped pores [12]. The hysteresis is more prominent in the case of the composite rGO/nC that can be attributed to the presence of the rGO component with 2D layered structure. The initial GtO material appeared non-porous with very low specific surface area (Table 1).

Table 1: The BET specific surface area (SSA_{BET}), total pore volume (TPV) and main pores' diameter (MPD) of the prepared materials

	Initial GtO	Pure nanocarbons	Composite rGO/nC
SSA_{BET} [m^2/g]	12	417	486
TPV [cm^3/g]	0.016	1.132	1.562
MPD. [nm]	3.2	3.8	4

The SSA of the composite rGO/nC increased significantly in comparison to the initial GtO reaching the value $486 m^2/g$ that is also higher than the SSA of the pure nC, with the TPT to follow the same trend. From the pore size distribution plots it is evident that the majority of the pores for all the samples have diameter between 3.2 and 4 nm. Also, a second population of pores with broad size distribution between 8 and 12 nm can be observed, which is less distinctive for the rGO/nC composite. This outcome may be related to the influence of the rGO component which hinders the aggregation of the nanocarbons and facilitates their homogeneous distribution. The high porosity of the rGO/nC composites makes them promising candidates for gas and/or energy storage applications.

4. Conclusions

Composite rGO/nanocarbons were successfully synthesized through a simultaneous reduction of solid graphite oxide and CO_2 gas at magnesiothermic conditions.

The XRD analysis evidenced the formation of nanocarbons for the pure nC and the composite rGO/nC. The initial GtO was not detected in the composite that was connected to its low content or to possible delamination/reduction during the treatment.

The SEM images demonstrated the delamination of the GtO and the presence of two types of morphologies for the composite, i.e. thin packs of layers and particles' aggregates attributed to the rGO and the nanocarbons, respectively.

The composite rGO/nC exhibited higher specific surface area ($486 m^2/g$) than the pure nC ($417 m^2/g$) that was related to influence of the rGO component hindering the aggregation of the formed nanocarbons.

5. Acknowledgments

The National Scientific Program "Petar Beron i NIE" contract number KII-06-ДБ/3 and "TIEDK-01729 CARBONGREEN" (MIS 5048538) co-financed by the European Union and Greek National Funds through the Operational Program Competitiveness, Entrepreneurship and Innovation, under the call RESEARCH-CREATE-INNOVATE are highly acknowledged.

6. References

1. A. Mondal, N.R. Jana, Rev. Nanoscience Nanotech. **3**, 177-193 (2014)
<https://doi.org/10.1166/rnn.2014.1051>
2. N. Devi, R. Kumar, S. Singh, R.K. Singh, Crit. Rev. Solid State Mater. Sci. (2022)
<https://doi.org/10.1080/10408436.2022.2132910>
3. V. Agarwal, P. Zetterlund, Chem. Eng. J. **405**, 127018 (2021)
<https://doi.org/10.1016/j.cej.2020.127018>
4. A. Ahmed, A. Singh, S.-J. Young, V. Gupta, M. Singh, S. Arya, Compos. Part A **165**, 107373 (2023)
<https://doi.org/10.1016/j.compositesa.2022.107373>
5. H. Zhang, X. Zhang, X. Sun, Y. Ma, Sci. Rep. **3**, article 3534 (2013)
<https://doi.org/10.1038/srep03534>
6. C. Luchetta, E.C.O. Munsignatti, H.O. Pastore, Front. Chem. Eng. **3**, 707855
<https://doi.org/10.3389/fceng.2021.707855>
7. T. Giannakopoulou, N. Todorova, N. Plakantonaki, M. Vagenas, I. Papailias, E. Sakellis, C. Trapalis, J. CO₂ Util. **65**, 102200 (2022)
<https://doi.org/10.1016/j.jcou.2022.102200>
8. J. Entwistle, A. Rennie, S. Patwardhan, J. Mat. Chem. A **6**, 18344-18356 (2018)
<https://doi.org/10.1039/c8ta06370b>
9. N. Todorova, T. Giannakopoulou, N. Boukos, E. Vermisoglou, C. Lekakou, C. Trapalis, Appl. Surf. Sci. **391**, 601-608 (2016)
<https://dx.doi.org/10.1016/j.apsusc.2016.04.088>
10. T. Giannakopoulou, N. Plakantonaki, M. Vagenas, I. Papailias, N. Boukos, N. Todorova, C. Trapalis, **17th**CEST, 00765 (2021)
https://cms.gnest.org/sites/default/files/Proceedings/cest2021_00765/cest2021_00765.pdf
11. E.C. Vermisoglou, T. Giannakopoulou, G.E. Romanos, N. Boukos, M. Giannouri, C. Lei, C. Lekakou, C. Trapalis, Appl. Surf. Sci. **358**, 110-121 (2015)
<https://doi.org/10.1016/j.apsusc.2015.08.123>
12. G. Leofanti, M. Padovan, G. Tozzola, B. Venturelli, Catal. Today **41**, 207-219 (1998)
[https://doi.org/10.1016/S0920-5861\(98\)00050-9](https://doi.org/10.1016/S0920-5861(98)00050-9)